Available online at www.sciencedirect.com
SCIENCE DIRECT®
ELSEVIER
International Journal of Solids and Structures 41 (2004) 6215–6232
INTERNATIONAL JOURNAL OF SOLIDS and STRUCTURES
www.elsevier.com/locate/ijsolstr

Experimental investigation of the transverse mechanical properties of a single Kevlar® KM2 fiber

Ming Cheng [a,*], Weinong Chen [a,*], Tusit Weerasooriya [b]

[a] *Department of Aerospace and Mechanical Engineering, The University of Arizona, 1130 N. Mountain, RM N614, Tucson, AZ 85721-0119, USA*

[b] *US Army Research Laboratory, Aberdeen Proving Ground, MD 21005-5066, USA*

Received 27 February 2004; received in revised form 6 May 2004
Available online 11 June 2004

Abstract

A new experimental setup is developed to investigate the transverse mechanical properties of Kevlar® KM2 fibers, which has been widely used in ballistic impact applications. Experimental results for large deformation reveal that the Kevlar® KM2 fibers possess nonlinear, pseudo-elastic transverse mechanical properties. A phenomenon similar to the Mullins effect (stress softening) in rubbers exists for the Kevlar® KM2 fibers. Large transverse deformation does not significantly reduce the longitudinal tensile load-bearing capacity of the fibers. In addition, longitudinal tensile loads stiffen the fibers' transverse nominal stress–strain behaviors at large transverse deformation. Loading rates have insignificant effects on their transverse mechanical properties even in the finite deformation range. An analytical relationship between transverse compressive force and displacement is derived at infinitesimal strain level. This relation is used to estimate the transverse elastic modulus of the Kevlar® KM2 fibers, which is 1.34 ± 0.35 GPa.

Keywords: Kevlar® KM2; Fiber; Mechanical properties; Large deformation; Loading rate

1. Introduction

The protection of military and law enforcement personnel from injury by high-velocity-object impact has created new challenges for fundamental scientific research since World War II and even more so recently. In particular, impact-energy-absorbing material development and characterization has become an imminent task for the scientific research community. As an important class of shock-absorbing materials, fabrics and flexible fibrous composites have been widely used in the bullet-proof vests and other body armor systems. Recent use of these materials in personnel protection applications creates an urgent need to develop a better

* Corresponding authors. Tel.: +1-520-6263159; fax: +1-520-6218191 (M. Cheng), Tel.: +1-520-621-6114; fax: +1-520-621-8191 (W. Chen).
E-mail addresses: mingc@u.arizona.edu (M. Cheng), weinong@u.arizona.edu (W. Chen).

0020-7683/$ - see front matter © 2004 Elsevier Ltd. All rights reserved.
doi:10.1016/j.ijsolstr.2004.05.016

scientific understanding of the mechanical response of these materials and the components made of these materials.

Kevlar® KM2 fabrics are widely used to produce personnel protection system because of their high stiffness, lightweight, and high strength. To understand the deformation process of a fabric armor system, many aspects such as material properties, fabric structure, projectile geometry, impact velocity, multiple ply interaction, far field boundary conditions and friction must be studied (Cheeseman and Bogetti, 2003). Among these factors, material properties are critical in determining the armor effectiveness.

In order to accurately simulate the ballistic performance of fabric armors for design purposes, many efforts have been focused on computational models to predict the resistance of fabrics to a high-velocity impact. For example, Taylor and Vinson (1990) proposed a ballistic fabric model that simulates the transverse impact by treating the fabric as a homogeneous, isotropic, elastic plate, which deforms into the shape of a straight-sided conical shell. However, this simple isotropic material model precludes the possibility of accurate simulation.

The earliest efforts in the attempt to predict ballistic impact effects on fabrics were those of Roylance et al. (1973) on biaxial fabrics. Fabrics are composite materials that offer significant computational challenges. The stress–strain behavior of these materials is generally nonlinear as well as anisotropic. Since there are few experimental investigations on these materials, many models assume a simple linear stress–strain relationship (Parga-Landa and Hernandez-Olivares, 1995; Roylance et al., 1995). In order to overcome this problem, Lim et al. (2003) employed a three-element spring-dashpot model to describe a rate-dependent nonlinear stress–strain behavior of Twaron fabric in their finite-element modeling study. They also accepted a failure criterion (Shim et al., 2001) that specifies the rate-dependent failure strain.

During impact, fibers are subjected to transverse compressive loading while they are being extended (tensile loading). Therefore, it is essential to obtain tensile behaviors of the fibers with transverse compressive loading superimposed on the fibers. However, few numerical models include the transverse behaviors of the fabric materials into account because of the lack of experimental investigations on this issue. Cunniff and Ting (1999) recognized this problem. They developed a numerical model to characterize the ballistic behavior of fabrics with warp and fill yarn elements modeled independently as elastic rod elements. Coupling between these elements was modeled with transverse spring elements corresponding to physical crossover. A nonlinear model with three empirical constants was used to describe the transverse behavior of the yarns.

Kevlar® KM2 fabrics and their ballistic application have recently been a research focus for many investigators (Johnson et al., 1999; Johnson et al., 2002). In order to obtain accurate information about the transverse behavior of yarns that will feed into these types of simulations, the behavior of their constituent, single fiber, is necessary to be examined first. As a first step to fulfill an accurate finite element simulation for ballistic impact, this paper discusses the development of a new experimental technique to investigate the transverse behavior of a Kevlar® KM2 single fiber. With this experimental technique, experiments were conducted with different loading arrangements on the Kevlar® KM2 single fiber to study the effects on the transverse compressive behavior under various conditions such as different loading rates, pre-tension in longitudinal direction, and cyclic transverse loading with increasing strain amplitudes. Finally, the experimental results in a small strain range are used to estimate the transverse elastic Young's modulus through the development of a relation between transverse compressive load and displacement.

2. Experiments

Because of the highly oriented chain molecules or crystals along the fiber axis, high-performance fibers, such as Kevlar® KM2 fibers, exhibit strong anisotropy. Since the properties have no significant deviation among directions perpendicular to the fiber axis, high-performance fibers are usually considered trans-

versely isotropic. The Young's modulus in the longitudinal direction (fiber axis direction) is much higher than that in the transverse direction (Kawabata, 1990). In addition, the stress–strain relation in the transverse direction is not necessarily linear in the case of large deformation.

The longitudinal behavior of a single fiber has been studied for a long time, and many test standards have been developed for this purpose, such as ASTM D3822-96 (Standard Test Method for Tensile Properties of Single Textile Fibers) and ASTM D3379-75 (Standard Test Method for Tensile Strength and Young's Modulus for High-Modulus Single-Filament Materials). However, the stress state in a fiber subjected to transverse impact is multi-axial. It is thus necessary to study the fiber response to mechanical loads in other directions such as transverse, in addition to the longitudinal direction. In the next section of this paper, the experimental technique that is developed to study the transverse mechanical behavior of the Kevlar® KM2 fibers is discussed.

2.1. Experimental setup

In order to investigate the transverse behavior of a single fiber, a new experimental setup was built. The main features of the new experimental setup are schematically shown in Fig. 1. With this arrangement, longitudinal tension of various levels can be applied to the fiber while being compressed transversely. In this figure, however, the devices that apply the longitudinal tension to the fiber specimen are not shown for the sake of clarity. The purpose to apply longitudinal tension to the fiber specimen is to investigate the effects of longitudinal tension on its transverse behavior. It also provides a possibility to estimate one of the Poisson's ratios of the fiber, which will be discussed later.

As shown in Fig. 1, the loading system includes a piezoelectric translator (PZT)—Physik Instrumente, model P840.10—which is driven by a LVPZT amplifier (model E-660). A push-rod is connected to the tip of the piezoelectric translator. This applies the transverse compressive load on the fiber specimen lying on a flat end of a supporting rod. Both the push-rod and supporting rod of 3.40 mm in diameter are made of silicon carbide (SiC). Young's modulus of silicon carbide is 420 GPa, much higher than that of general high-performance fibers, such as Kevlar® KM2 fibers, in transverse direction. Therefore, the deformation in the test jig is negligible compared to that of fiber. The loading tip of the push rod is tapered from a circular cross-section to a rectangular shape to form a contact surface of 1.6 mm in width as shown in the sectional

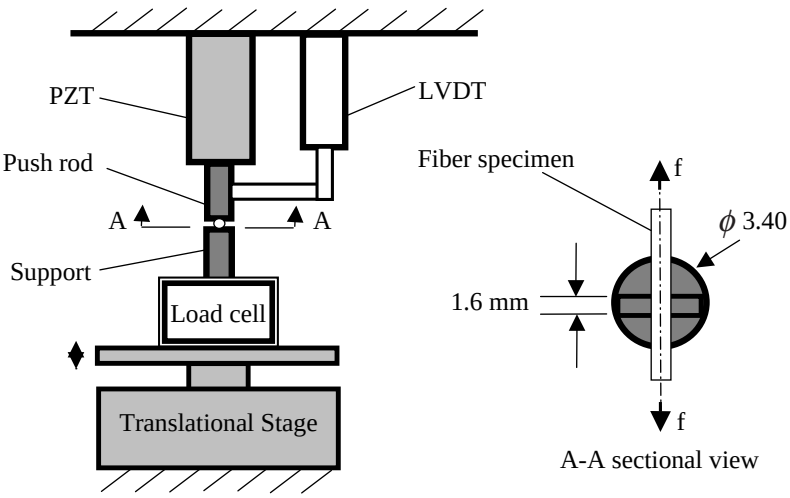

Fig. 1. Schematic description of the experimental setup for transverse compressive tests.

view of Fig. 1. This bottom contact surface of the push-rod and the top surface of the supporting rod are polished with a 0.3 μm de-agglomerated alumina polishing suspension.

The compressive load is sensed by an INTERFACE Load cell (model 1500ASK-50), which is positioned under the supporting rod. This load cell is a strain gage force transducer with a capacity of 222.4 N (50 lb). This capacity is much higher than the maximum load observed in the single fiber tests. However, it provides a strong support with its relative high stiffness to avoid significant longitudinal deformation in the load cell, thus reducing the errors that may occur in the measurement of fiber deformation. The small load signal is conditioned with a Vishay Measurements Group 2311 signal conditioning amplifier to a level acceptable for an analog-to-digital converter (ADC). The displacement is measured using a linear variable displacement transducer (LVDT). The displacement signal from FASTAR® linear displacement transducer (SENTECH, Inc., model FS380, connected to a model SP300A signal processor) is also sampled with another channel of the ADC converter. A MELLES GRIOT vertical translational stage (model 07 TEZ 007) is used to facilitate the proper positioning and alignment of these components. The driving signal for the piezoelectric translator and data acquisition of load and displacement signals are controlled by a computer. This computer as well as signal conditioners is not shown in Fig. 1.

2.2. Specimens

The specimens are of 850 denier Kevlar® KM2 fibers from DuPont. The density of these fibers is 1440 kg/m^3. The diameter (D) of the Kevlar® KM2 fiber is determined using a scanning electronic microscope (SEM) and is 12 μm, which is the same value provided by the manufacturer. A SEM micrograph of Kevlar® KM2 fibers is given in Fig. 2, which shows little variation in diameter along the fiber axis.

2.3. Experimental results

The transverse experimental procedure is similar to a normal uniaxial compressive test method used for a standard material specimen. A fiber is loaded between the push-rod and supporting rod. For tests involved with studying the effects of longitudinal tension, longitudinal loading is applied using a Teflon pulley system and dead weights. The computer, by sending a cyclic triangular signal to the piezoelectric translator system, applies a monotonically increasing and then decreasing transverse loading to the specimen. These ramp loading and unloading are applied at the same rate. The computer also simultaneously records the linear

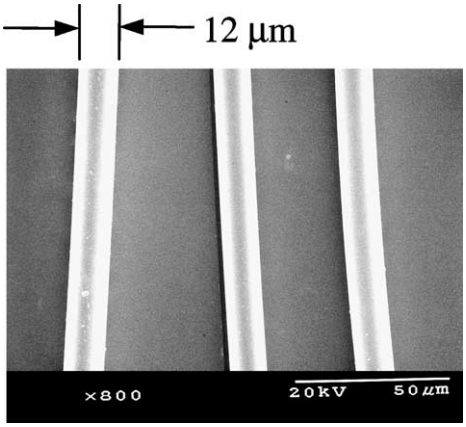

Fig. 2. A SEM micrograph of the Kevlar® KM2 fibers.

displacement signal from the LVDT and compressive load signal from the load cell. The recorded signals are later analyzed to obtain the stress–strain behavior of the fiber.

In the following, the experimental results with different loading types are presented and discussed to obtain an overall view of the transverse mechanical behavior of the Kevlar® KM2 fibers.

2.3.1. Transverse compressive behavior without longitudinal loading

Fig. 3 is a typical load–deformation curve obtained from a test on a Kevlar® KM2 fiber with cycling of displacement at a constant amplitude. In Fig. 3, the ordinate is nominal compressive stress, which is defined as push load per unit of length in longitudinal direction divided by the diameter of the fiber. Abscissa is the displacement of the bottom surface of the push-rod normalized by the diameter of the fiber specimen. In this paper, the normalized displacement is called nominal strain, when its value at the initial point of the push-rod touching the fiber is subtracted from data so that this value is zero at the beginning of loading. The insert in Fig. 3 is the time history of the displacement.

Because of unavoidable dust particles in the air and our inability to consistently keep the fiber perfectly straight at the beginning, initial loading point is difficult to obtain. Therefore, the test results are not necessarily reliable at the initial stage of the experiments when the longitudinal tension loading is not present. This situation is significantly improved once a longitudinal tensile loading is applied, which straightens the fiber. Experimental results with pre-tension in longitudinal direction are discussed in Section 2.3.4. In the case of ambiguous initial stage of transverse compression, the normalized displacement is used for deformation instead of nominal strain. Fig. 3 is a response function of the fiber transverse structure, not a true strain vs. true stress curve. However, it still reveals the transverse response of this material.

A Kevlar® KM2 fiber may be approximately considered linear elastic in its transverse direction at an infinitesimal deformation range. However, the overall behavior in a large deformation range is obviously nonlinear and nonelastic. As shown in Fig. 3, the first loading path from its virgin state to a nominal strain of about 0.48 is nonlinear (note that the zero nominal strain is located at a normalized displacement of 0.27

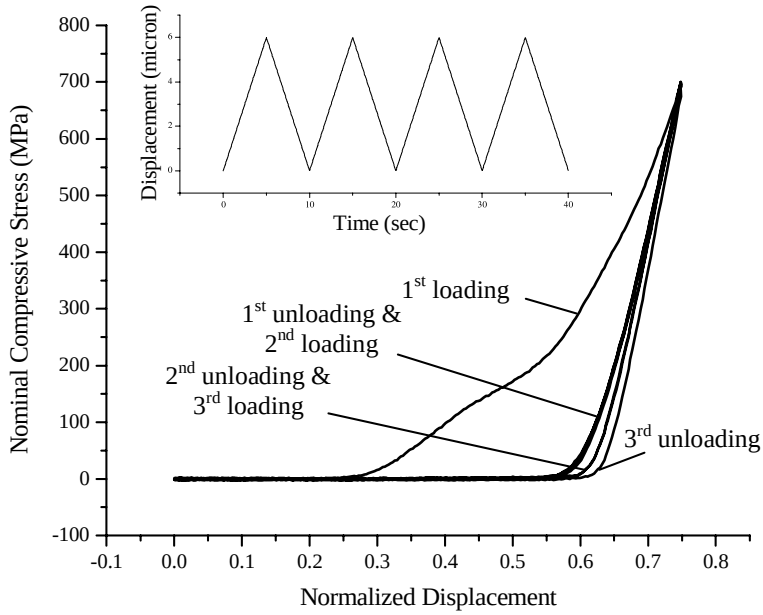

Fig. 3. Cyclic transverse loading of a Kevlar® KM2 fiber at a nominal strain rate of 0.075/s.

in Fig. 3). An unloading from this nominal strain, which corresponding to a normalized displacement of 0.75, hardly recovers its full deformation, leaving a large residual strain of 0.30 in terms of nominal strain. Observation with an optical microscope shows that the fiber remains its deformed shape even two months after it is transversely pressed. Once this fiber is loaded again, the second and later loading and unloading paths follow the first unloading path with some small deviation from it. This property is refereed to as pseudo-elastic by Ogden (2001) in rubber materials, which makes the Kevlar® KM2 fibers an efficient energy-absorbing material during initial loading from virgin states. By integration over one loading and unloading cycle, the energy absorbed by one Kevlar® KM2 fiber at a nominal maximum strain of 0.48 is about 9 μJ/m of fiber length when the fiber is loaded transversely.

2.3.2. Longitudinal tensile behavior after transverse loading and unloading of fibers

Furthermore, the large residual strain caused by the transverse compression does not reduce the loading capacity of the fiber in its longitudinal direction. A series of tests are completed to measure the fibers' longitudinal mechanical behavior after they are transversely compressed to a nominal strain of 0.48. These longitudinal tensile tests follow the method introduced in ASTM D3379-75 with a gage length of 10 mm for the fiber specimen. Table 1 lists the longitudinal tensile test results of both transversely compressed and uncompressed fiber specimens. The 95% confidence intervals of these results are estimated from 25 tests under each test condition. By taking the scatter of test results into account, the difference in the longitudinal tensile behavior of the Kevlar® KM2 fibers is insignificant. In the ballistic applications, this property may be a significant advantage. Once an object impacts a fiber transversely and causes large deformation, the fiber can still maintain its load-bearing capability in its longitudinal direction and spread the impact loads, which is the main energy-absorption source since the transverse deformation is limited due to the tiny size of diameter.

2.3.3. Effects of loading rates on transverse behavior in the absence of longitudinal loading

The Kevlar® KM2 fiber is widely used for ballistic impact application. The effects of loading-rate on its mechanical properties are another major concern. With the new experimental facility, a series of tests with different loading rates are performed, the results of which are shown in Fig. 4. At the quasi-static loading rate range from 0.00075/s to 0.075/s in terms of nominal strain per second, the loading rate effects on the transverse mechanical properties of the Kevlar® KM2 fiber are insignificant. This result is not totally unexpected. Loading rate effects in polymers come close to a glass-to-rubber transition. This is when a stiff mode of deformation is giving way to a softer mode. At slow rates this happens more easily than at high rates. However, there is no such transition in Kevlar® KM2 near room temperature (Hearle, 2003). This property is consistent with the longitudinal mechanical behavior of the Kevlar® KM2 fibers. The longitudinal mechanical behavior of the Kevlar® KM2 fibers at a strain rate of 1500/s, which was obtained from experiments using a modified split Hopkinson tension bar (SHTB) technique, has insignificant difference from that of quasi-static loading. Dynamic longitudinal mechanical behavior of the Kevlar® KM2 fibers with the modified SHTB experiments will be reported in a separate paper by the authors.

Table 1
Longitudinal tensile properties of transversely compressed and uncompressed fibers

	Uncompressed	Compressed
Young's modulus (GPa)	84.62 ± 4.18	81.08 ± 4.20
Strength (GPa)	3.88 ± 0.40	3.64 ± 0.34
Failure strain (%)	4.52 ± 0.37	4.58 ± 0.37

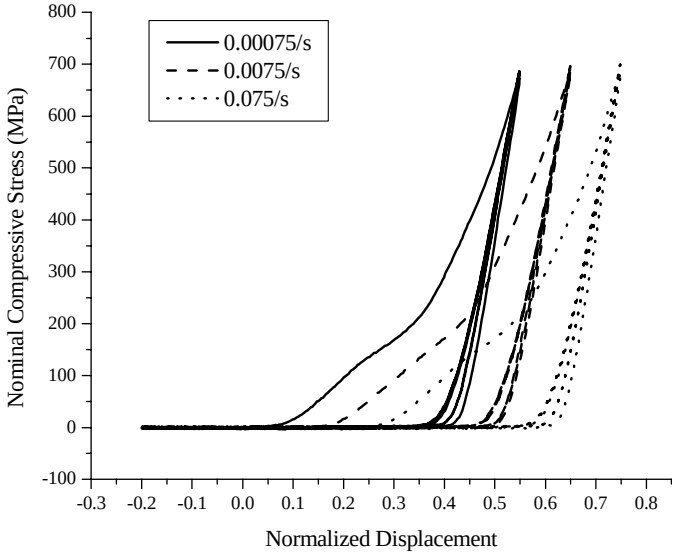

Fig. 4. Effects of loading rate.

2.3.4. Transverse compressive behavior of longitudinally pre-tensioned fibers

In the large deformation range, the Kevlar® KM2 fibers do not follow linear elastic behavior as verified by the results in Figs. 3 and 4. The superposition principle is therefore invalid when the fiber is applied with a multi-axial loading. To quantify the fiber performance under transverse impact, it is important to understand the interactions between the longitudinal and transverse mechanical properties. Therefore, another series of experiments are conducted to investigate the effects of longitudinal loading on the fiber's transverse properties. Fig. 5 shows the test results with three different levels of longitudinal pre-loading. The pre-loading in tension in the longitudinal direction is feasible because there is no friction between loading platens and the fiber in this case. Friction is inevitable when performing longitudinal tension tests with transverse pre-loading in compression. Transverse compression must be applied through a contact area of the fiber and the lateral loading platens. Friction is then involved in this contact zone. This friction problem prevents the studying of material behavior when both longitudinal and transverse loading is applied simultaneously.

The results in Fig. 5 indicate that the effects of longitudinal tensions on the transverse mechanical properties of the Kevlar® KM2 fibers are insignificant at small deformation range (nominal strain less than 0.1), though the first loading curve at its infinitesimal deformation with free longitudinal tension may not be reliable because of the ambiguity of the initial contact stage. However, the effects at large deformation (nominal strain larger than 0.1) cannot be ignored. The longitudinal tension increases the transverse stiffness of the Kevlar® KM2 fiber. The nominal compressive stress increases as the longitudinal tension increases for the same nominal transverse strain. So, when an object impacts a Kevlar® KM2 fiber transversely, the transverse deflection causes the longitudinal tension response to increase. This then stiffens the fiber transversely, enhancing the energy-absorption capacity of the fiber.

2.3.5. Effect of increasing amplitude of transverse loading cycles

From above experimental results, it is clear that the first nominal compressive stress vs. normalized displacement curve in transverse direction is much different from those curves obtained from reloading the same specimen. The first loading and unloading cycle is the most energy-absorbing cycle, and causes larger

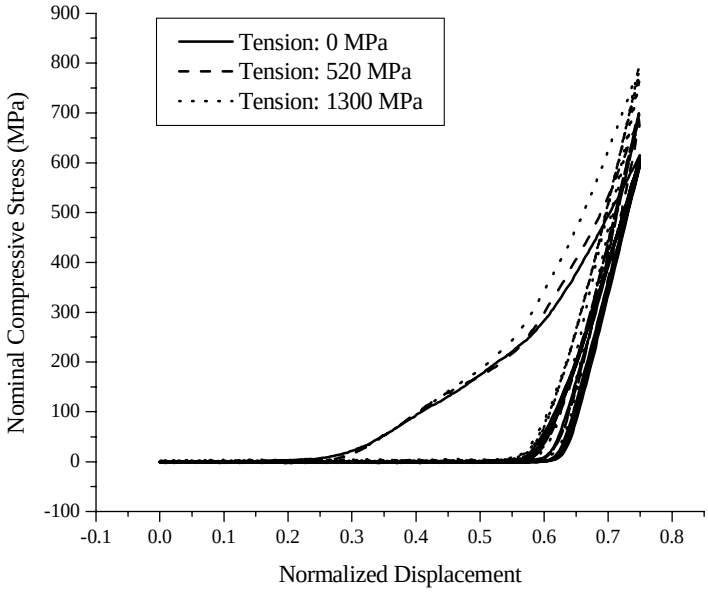

Fig. 5. Effects of pre-tension in longitudinal direction.

residual strain in unloading. The observed differences in the following loading and unloading paths are not significant comparing to differences observed between the first cycle and the following loading cycles if their maximum nominal strains do not exceed the first one. In order to reveal the mechanical behavior of later loading cycles when their maximum nominal strains exceed the previous maxima, a series of experiments were conducted with sets of four cycles where the nominal strain amplitude of each set of cycles gradually increases. The results of these successive loading cycles are shown in Fig. 6 with an insert to describe the

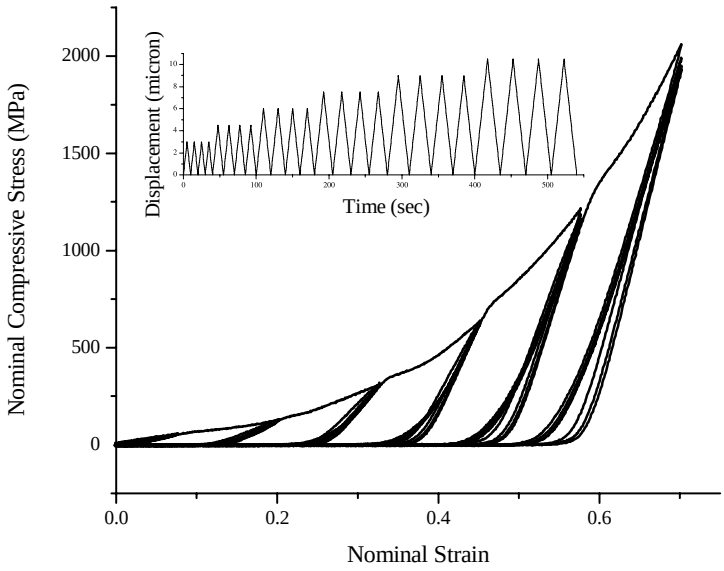

Fig. 6. Successive loading cycles with step increasing nominal strains.

time history of loading cycles. In these experiments, each loading–unloading cycle with same amplitude consists of four sub cycles of loading–unloading cycles.

The results in Fig. 6 show that large residual strain exists even at a small strain level after the first sub cycle in the first-cycle. The amplitude of the first four loading and unloading sub-cycles is 0.075 in terms of nominal strain. The observed transverse mechanical behavior for the cycles is the same as for experiments showed in Fig. 3. After these initial four successive sub-cycles, the next loading cycle can be divided into two stages. The first stage, with nominal strain less than previous maximum nominal strain, which is 0.075, follows the fourth loading sub-cycle. However, once the first loading sub-cycle of the second loading cycle exceeds the previous maximum nominal strain, it turns to a loading path that a virgin specimen is expected to follow. The fifth unloading path (unloading of first sub-cycle in the second cycle) leaves an even larger residual strain, causing large energy absorption. The later loading and unloading cycles follows the fifth unloading path until the ninth loading (first sub-cycle of the third loading cycle), which is another new loading with maximum nominal strain exceeding previous maximum nominal strain. This phenomenon is similar to the Mullins effect, which was found in many rubber materials (Mullins, 1969; Cheng and Chen, 2003). Ogden's pseudo-elasticity theory for an idealized Mullins effect could be employed to model this phenomenon (Ogden and Roxburgh, 1999a,b; Dorfmann and Ogden, 2004). This modeling effort will be reported in a separate paper by the authors.

3. Estimation of elastic modulus in transverse direction

The experimental results at small nominal strains can be used to estimate the elastic modulus (Young's modulus) in the transverse direction.

Hadley et al. (1965) are the pioneers in the experimental determination of transverse Young's modulus of fibers. They compressed a fiber between two rigid parallel transparent flats. The amount of flattening of the contact area of the fiber was measured by a microscope as a function of compressive load. The transverse Young's modulus was then estimated from a relation between contact area and compressive force through an analytical solution to this plane strain problem. Later, Pinnock et al. (1966), in the same research group, employed the same experimental setup, but measured the change in fiber diameter parallel to the plane of the flats as a function of compressive load. They developed another analytical method to estimate the transverse Young's modulus of fibers from those experimental measurements. Although both methods were used on polyethylene terephthalate and nylon, the measurements could not be obtained very accurately (Pinnock et al., 1966). Application of these two methods requires measurement of the contact width or diametrical change with a microscope. The diameter of modern high-performance fibers is usually between 5 and 15 μm. It is difficult to obtain accurate measurement of contact width or diametrical changes for these fine fibers.

The transverse Young's modulus of single fiber can also be obtained by measuring transverse load–displacement curve of the fiber. Kawabata (1990) developed an instrument to obtain transverse load–displacement curve using the same experimental concept as ours with different driving and measuring techniques. He placed a fiber on a flat steel bed. In his method, a push-rod of a square bottom of 0.2×0.2 mm^2 was driven by an electromagnetic power driver towards the fiber. The compressive load and displacement were measured through a force transducer and a linear differential transformer mounted on the push-rod. A relationship between the compressive load and displacement associated with a fiber was employed to estimate the transverse Young's modulus. The relationship they used was claimed to be cited from the works of Hadley et al. (1965) and Pinnock et al. (1966). However, Hadley et al. (1965) and Pinnock et al. (1966) did not give such a relationship explicitly. The authors of the current research thus could not verify the validity and accuracy of the relationship. In this paper, an explicit relation between the

driving force and displacement is derived to estimate the transverse Young's modulus of the Kevlar® KM2 fiber.

3.1. Theoretical analysis

Since the length of the contact zone (1.6 mm) is much larger than the diameter of the fiber (12 μm), the problem is formulated as a plane strain problem. Furthermore, the contact zones are assumed to be flat because the Young's modulus of the push rod and support material (SiC), 420 GPa, is much higher than the longitudinal Young's modulus of the fiber (about 90 GPa). Longitudinal modulus is about one order of magnitude higher than its transverse Young's modulus (Kawabata, 1990). The distortions of the push rod and support are neglected. The cross sectional views of the Kevlar® KM2 fiber in its original and deformed states are depicted in Fig. 7. Notations used in the following derivations are also identified in the figure. The longitudinal direction, x_3, is perpendicular to the paper in this diagram.

Without considering body forces and frictions in the contact zones, this case of plane strain problem can be described by the following equations of equilibrium.

$$\sigma_{\beta\alpha,\beta} = 0 \quad \alpha, \beta = 1, 2 \tag{1}$$

$$\sigma_{33,3} = 0 \tag{2}$$

Outside the contact zones, boundaries of the cylinder are in a stress-free state. However, within the contact zones, the sum of the vertical stresses in the contact zones must be equal to the compressive load,

$$\int_{-b}^{+b} \sigma_{22}\,\mathrm{d}x_1 = -F \tag{3}$$

and the effects of friction in contact zones are ignored,

$$\sigma_{12} = 0 \tag{4}$$

In Eq. (3), F stands for the transverse compressive load per unit length along the fiber axial direction.

This plane strain problem has been analytically solved by McEwen (1949) in the case of isotropic materials by employment of a complex variable method. According to his method, if the real (Φ) and imaginary (Ψ) parts of a complex analytic function, Γ, separately satisfy Laplace's equation in the x_1–x_2 plane and possess the following relations:

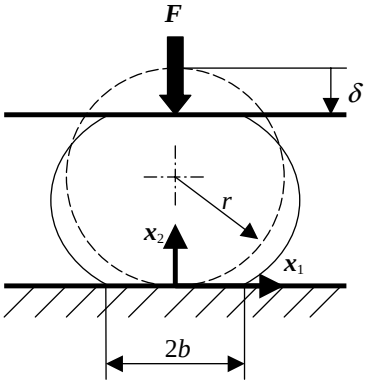

Fig. 7. Transverse compression of a single fiber.

$$\Phi_{,1} = \Psi_{,2}, \quad \Phi_{,2} = -\Psi_{,1} \tag{5}$$

the following stress set forms a general solution to the above plane strain problem.

$$\sigma_{11} = \Phi - x_2\Psi_{,1} \tag{6a}$$

$$\sigma_{22} = \Phi + x_2\Psi_{,1} \tag{6b}$$

and

$$\sigma_{12} = -x_2\Psi_{,2} \tag{6c}$$

For elastic cylinders in contact along a generatrix, the plane strain problem with our specific boundary conditions, McEwen (1949) proposed an analytic function.

$$\Gamma = -\frac{2F}{\pi b^2}\left[\sqrt{b^2 - (x_1 + \mathrm{i}x_2)^2} + \mathrm{i}(x_1 + \mathrm{i}x_2)\right] \tag{7}$$

where b is the half width of the contact zone shown in Fig. 3.

In order to establish a relationship between the compressive load F and the transverse displacement δ of a high-performance fiber, we employ McEwen's stress solution, Eq. (7), and use the constitutive relation for transverse isotropic materials. The overall displacement is the accumulation of strains along x_2-axis,

$$\delta = -2\int_0^r (u_{2,2})_{x_1=0}\,\mathrm{d}x_2 \tag{8}$$

The normal strain distribution along the vertical direction when $x_1 = 0$ must then be explicitly expressed in order to obtain the displacement δ from Eq. (8).

A Kevlar KM2 fiber may be treated as a transversely isotropic material because of its highly oriented chain of molecules. With x_3-axis as the axis of transversely isotropic, the constitutive relations for a linear elastic body are

$$\begin{Bmatrix} \varepsilon_{11} \\ \varepsilon_{22} \\ \varepsilon_{33} \\ \varepsilon_{23} \\ \varepsilon_{31} \\ \varepsilon_{12} \end{Bmatrix} = \begin{bmatrix} S_{11} & S_{12} & S_{13} & 0 & 0 & 0 \\ S_{12} & S_{11} & S_{13} & 0 & 0 & 0 \\ S_{13} & S_{13} & S_{33} & 0 & 0 & 0 \\ 0 & 0 & 0 & 0.5S_{44} & 0 & 0 \\ 0 & 0 & 0 & 0 & 0.5S_{44} & 0 \\ 0 & 0 & 0 & 0 & 0 & S_{11} - S_{12} \end{bmatrix} \begin{Bmatrix} \sigma_{11} \\ \sigma_{22} \\ \sigma_{33} \\ \sigma_{23} \\ \sigma_{31} \\ \sigma_{12} \end{Bmatrix} \tag{9}$$

in terms of the five independent compliance constants. Therefore, we get

$$u_{2,2} = \varepsilon_{22} = S_{12}\sigma_{11} + S_{11}\sigma_{22} + S_{13}\sigma_{33} \tag{10}$$

and

$$u_{3,3} = \varepsilon_{33} = S_{13}\sigma_{11} + S_{13}\sigma_{22} + S_{33}\sigma_{33} \tag{11}$$

In the case of plane strain, $u_{3,3} = 0$. Therefore

$$\sigma_{33} = -\frac{S_{13}}{S_{33}}(\sigma_{11} + \sigma_{22}) \tag{12}$$

By substitution of Eqs. (5), (6) and (12) into Eq. (10), we get

$$u_{2,2} = \left(S_{11} + S_{12} - \frac{2S_{13}^2}{S_{33}}\right)\Phi - (S_{11} - S_{12})x_2\Phi_{,2} \tag{13}$$

Because what we concern is the normal strain distribution along the vertical direction when $x_1 = 0$, we pay particular attention on the solution when $x_1 = 0$.

$$(\Gamma)_{x_1=0} = -\frac{2F}{\pi b^2}\left(\sqrt{b^2+x_2^2} - x_2\right) \tag{14}$$

$$(\Phi)_{x_1=0} = -\frac{2F}{\pi b^2}\left(\sqrt{b^2+x_2^2} - x_2\right) \tag{15}$$

and

$$(\Psi)_{x_1=0} = 0 \tag{16}$$

Substitute Eq. (15) into Eq. (13), we then obtain,

$$(u_{2,2})_{x_1=0} = -\frac{2F}{\pi b^2}\left[\left(S_{11}+S_{12}-\frac{2S_{13}^2}{S_{33}}\right)\left(\sqrt{b^2+x_2^2}-x_2\right) + (S_{11}-S_{12})x_2\frac{\sqrt{b^2+x_2^2}-x_2}{\sqrt{b^2+x_2^2}}\right] \tag{17}$$

Therefore, the relation between the load F and displacement δ is created as

$$\delta = \frac{4F}{\pi b^2}\left[\left(S_{12}-\frac{S_{13}^2}{S_{33}}\right)\left(\sqrt{b^2+r^2}-r\right)r + \left(S_{11}-\frac{S_{13}^2}{S_{33}}\right)b^2\ln\frac{\sqrt{b^2+r^2}+r}{b}\right] \tag{18}$$

Next, the half width of contact zone must be determined. Within the contact zones, the curvature of the cylinder before loading is $1/r$, which is reduced to zero by the load. This means the stress distribution within the contact zone produces a change of curvature of $-1/r$, which is related to the displacement in the contact zone as follows.

$$u_{2,11} = -\frac{1}{r} \tag{19}$$

We will use this relation to determine the value of b. From Eq. (9), we know

$$u_{1,2} + u_{2,1} = 2(S_{11} - S_{12})\sigma_{12} \tag{20}$$

Therefore, by differentiating both sides of Eq. (20) with x_1

$$u_{1,21} + u_{2,11} = 2(S_{11} - S_{12})(-x_2\Psi_{,21}) \tag{21}$$

From Eq. (9), we also know

$$u_{1,1} = S_{11}\sigma_{11} + S_{12}\sigma_{22} + S_{13}\sigma_{33} = \left(S_{11}+S_{12}-\frac{2S_{13}^2}{S_{33}}\right)\Phi - (S_{11}-S_{12})x_2\Psi_{,1} \tag{22}$$

By differentiating both sides of Eq. (22) with x_2 we get

$$\begin{aligned} u_{1,21} &= \left(S_{11}+S_{12}-\frac{2S_{13}^2}{S_{33}}\right)\Phi_{,2} - (S_{11}-S_{12})\Psi_{,1} - (S_{11}-S_{12})x_2\Psi_{,12} \\ &= \left(S_{11}+S_{12}-\frac{2S_{13}^2}{S_{33}}\right)(-\Psi_{,1}) - (S_{11}-S_{12})\Psi_{,1} - (S_{11}-S_{12})x_2\Phi_{,11} \\ &= \left(-2S_{11}+\frac{2S_{13}^2}{S_{33}}\right)\Psi_{,1} - (S_{11}-S_{12})x_2\Phi_{,11} \end{aligned}$$

Substituting the above result into Eq. (21),

$$\begin{aligned} u_{2,11} &= -2(S_{11}-S_{12})x_2\Phi_{,11} - \left(-2S_{11}+\frac{2S_{13}^2}{S_{33}}\right)\Psi_{,1} + (S_{11}-S_{12})x_2\Phi_{,11} \\ &= 2\left(S_{11}-\frac{S_{13}^2}{S_{33}}\right)\Psi_{,1} - (S_{11}-S_{12})x_2\Phi_{,11} \end{aligned} \tag{23}$$

In the lower contact zone, where $x_2 = 0$,

$$\Gamma = -\frac{2F}{\pi b^2}\left[\sqrt{b^2-x_1^2} + \mathrm{i}x_1\right] \tag{24}$$

$$\Phi = -\frac{2F}{\pi b^2}\sqrt{b^2-x_1^2} \tag{25}$$

$$\Psi = -\frac{2F}{\pi b^2}x_1 \tag{26}$$

So, by plug Eqs. (25) and (26) into Eq. (23) and use Eq. (19),

$$(u_{2,11})_{x_2=0} = -\frac{4F}{\pi b^2}\left(S_{11}-\frac{S_{13}^2}{S_{33}}\right) = -\frac{1}{r} \tag{27}$$

Finally, the half width of the contact zone is

$$b = \sqrt{\frac{4Fr}{\pi}\left(S_{11}-\frac{S_{13}^2}{S_{33}}\right)} \tag{28}$$

The compliance constants can be expressed with Young's moduli and Poisson's ratios as follows:

$$S_{11} = \frac{1}{E_1} \tag{29}$$

$$S_{12} = -\frac{v_{12}}{E_1} \tag{30}$$

$$S_{13} = -\frac{v_{13}}{E_1} = -\frac{v_{31}}{E_3} \tag{31}$$

and

$$S_{33} = \frac{1}{E_3} \tag{32}$$

Therefore, the final relation between displacement and load is

$$\delta = \frac{4F}{\pi b^2}\left[\left(-\frac{v_{12}}{E_1}-\frac{v_{31}^2}{E_3}\right)(\sqrt{b^2+r^2}-r)r + \left(\frac{1}{E_1}-\frac{v_{31}^2}{E_3}\right)b^2\ln\frac{\sqrt{b^2+r^2}+r}{b}\right] \tag{33}$$

with

$$b = \sqrt{\frac{4Fr}{\pi}\left(\frac{1}{E_1}-\frac{v_{31}^2}{E_3}\right)} \tag{34}$$

If we normalized the load (F) and displacement (δ) by the diameter of the fiber to give them units of stress and strain respectively, the above relation is then as follows.

$$\bar{\varepsilon} = \frac{4\bar{\sigma}}{\pi b^2}\left[\left(-\frac{v_{12}}{E_1} - \frac{v_{31}^2}{E_3}\right)(\sqrt{b^2+r^2} - r)r + \left(\frac{1}{E_1} - \frac{v_{31}^2}{E_3}\right)b^2 \ln\frac{\sqrt{b^2+r^2}+r}{b}\right] \tag{35}$$

with

$$b = \sqrt{\frac{8\bar{\sigma}r^2}{\pi}\left(\frac{1}{E_1} - \frac{v_{31}^2}{E_3}\right)} \tag{36}$$

where

$$\bar{\sigma} = \frac{F}{D} \tag{37}$$

and

$$\bar{\varepsilon} = \frac{\delta}{D} \tag{38}$$

are referred as to nominal transverse stress and nominal transverse strain.

3.2. Estimation of elastic parameters

Eq. (35) is used to estimate the transverse Young's modulus of the Kevlar® KM2 fibers. Before this application, a calibration test is performed with a 24 carat gold fiber. This gold fiber is an isotropic material with a diameter of 50.8 μm. Experimental results show that the Young's modulus is 76.05 GPa, which is within the range of 75.98–81.02 GPa (Granta Design Limited, http://www.grantadesign.com). This calibration test confirms the applicability of the relation between the load F and displacement δ, Eq. (33), as well as the validity of our experimental facility.

To estimate the transverse Young's modulus of the Kevlar® KM2 fibers using Eq. (35), there are other parameters that need to be known: fiber diameter, longitudinal Young's modulus, and two Poisson's ratios.

The diameter (D) of the Kevlar® KM2 fiber is determined with a scanning electron microscope (SEM) to be 12 μm (from Fig. 2), the same as that provided by the manufacturer.

A MTS 810 material testing machine, working at a displacement control mode, is used to test the Kevlar® KM2 fibers in its longitudinal direction. Results show that the Kevlar® KM2 fibers exhibit linear stress–strain behavior to failure in their longitudinal direction. The Young's modulus in the longitudinal direction (E_3) is 84.62 ± 4.18 GPa, the range of which is 95% confidence interval. The strength of the Kevlar® KM2 fibers is 3.88 ± 0.40 GPa with a failure strain $4.52\% \pm 0.37\%$.

3.2.1. Estimation of Poisson's ratios

A Poisson's ratio, v_{ij}, is defined as the ratio of the negative of the normal strain in direction 'j' to the normal strain in direction 'i', when the only normal load is applied in direction 'i'. In order to estimate one of the Poisson's ratios, two transverse compressive tests are consecutively performed with an exactly same state of the test facility. The first test is performed without any longitudinal tension applied. Afterwards, a tensile stress of 1.3 GPa is applied in the longitudinal direction. The second test is performed at the location 5 mm away from the first loading site of the same fiber. Fig. 8 shows the results of these two tests.

The shift in displacement of the tip of the push rod reflects the shrink in the diameter of the fiber resulted from the longitudinal tension load provided that the diameters of these two test locations are the same. This

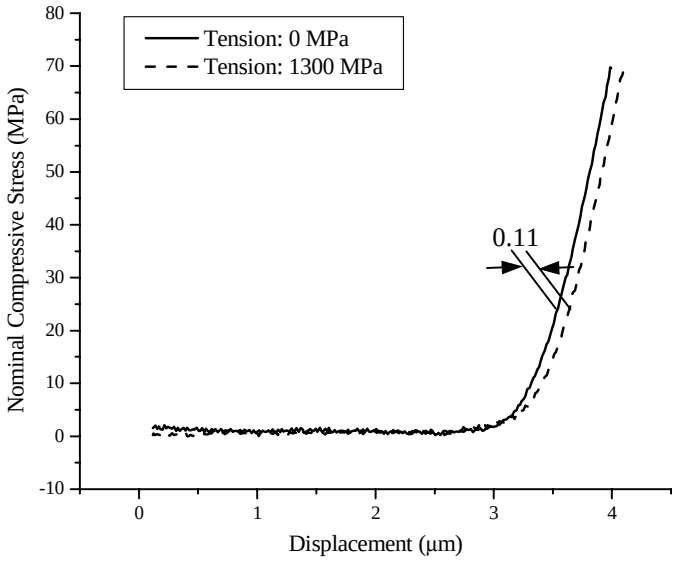

Fig. 8. Estimation of Poisson's ratio v_{31}.

is reasonable for the Kevlar® KM2 fibers within 5 mm vicinity. We can then estimate the Poisson's ratio as follows.

$$v_{31} = -\frac{E_3}{\sigma_3}\varepsilon_1 = -\frac{E_3}{\sigma_3}\frac{\Delta D}{D} \tag{39}$$

where ΔD is the change in diameter, which is 0.11 μm from data in Fig. 8. By this method, the Poisson's ratio, v_{31}, is determined to be 0.60 ± 0.08, which exceeds 0.5, the maximum value for isotropic materials. This is not a contradiction since the requirement on the basis of positive strain energy is (Kaw, 1997),

$$S_{11} + S_{12} > \frac{2S_{13}^2}{S_{33}} \tag{40}$$

which can be verified to be satisfied after the transverse Young's modulus is determined.

The Poisson's ratio, v_{12}, is difficult to estimate by current experimental technique on a single fiber specimen. Using the published data about other Kevlar® materials (Yang, 1992), a number of 0.24 is chosen for the estimation of the transverse Young's modulus. Numerical experiments reveal that the Poisson's ratios have insignificant effects on the estimation of the transverse Young's modulus. In the case of the Kevlar® KM2 fibers, the difference of the transverse Young's modulus is within 2% if the Poisson's ratio, v_{12}, is changed from 0.20 to 0.35. This difference is within the scatter range of tests.

3.2.2. Estimation of transverse Young's modulus of Kevlar® KM2 fibers

With the above parameters, the transverse compressive experimental results are curve-fitted into Eq. (35). Because of the ambiguity of the initial contact time when the fiber is in a tension free state and the insignificant effects of longitudinal tension on the transverse behavior at small strains (Fig. 5), experimental results with a longitudinal tension of 520 MPa are used for the estimation of the transverse Young's

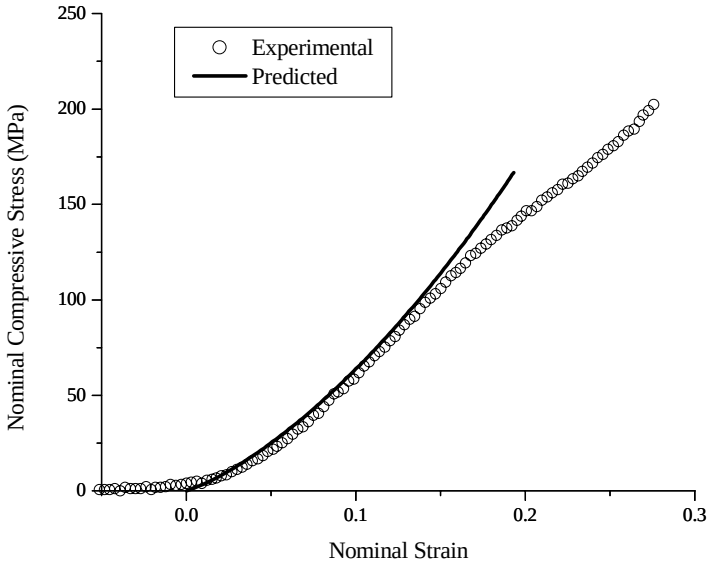

Fig. 9. Comparison between model prediction and experimental data.

modulus. Curve fitting results show that the Young's modulus of the Kevlar® KM2 fibers in their transverse direction (E_1) is 1.34 ± 0.35 GPa. A comparison between the model prediction and experimental data is shown in Fig. 9.

Fig. 9 shows that, Eq. (35) can predict the behavior of transverse displacement induced by transverse compressive load reasonably well on a first loading path until a nominal strain of at least 10%. Within large deformation range, structural nonlinearity must be considered.

4. Conclusions

A new experimental facility is developed to measure the transverse compressive behavior of Kevlar® KM2 fibers, which is transversely isotropic to the fiber axis with a diameter of 12 μm. A byproduct of this experimental facility is the capacity of estimating one of the Poisson's ratios associated with longitudinal loading.

The transverse compressive behavior of the Kevlar® KM2 fibers is nonlinear and pseudo-elastic. The original loading path is totally different from its unloading path and subsequent loading and unloading cycles, provided the maximum deformation of these loading and unloading cycles does not exceed the maximum deformation this specimen has experienced in the first loading cycle. The original loading and unloading cycle leaves a large residual strain in the fiber, causing large energy absorption, which is an advantage for ballistic impact resistance applications. Another advantage of the Kevlar® KM2 fibers is that, they keep their excellent mechanical properties in their longitudinal direction despite of large residual strain in transverse direction.

Phenomenon similar to the Mullins effect in rubber materials also exists in the transverse response of the Kevlar® KM2 fibers. Besides, the transverse compressive behavior of the Kevlar® KM2 fibers is insensitive to loading rates. However, the longitudinal tensions can stiffen the transverse behavior at large deformation although this effect is insignificant at small deformation.

In order to estimate the transverse Young's modulus of the Kevlar® KM2 fibers, a relation is derived between transverse compressive load and deflection based on a classical stress solution to this plane strain problem and the constitutive relation for transversely isotropic materials. With small deformation results from transverse compressive tests, the transverse Young's modulus of the Kevlar® KM2 fibers is estimated to be 1.34 ± 0.35 GPa.

Acknowledgements

This research was supported by US Army Research Laboratory (ARL) and US Army Natick Soldier Center through a cooperative agreement (DAAD19-02-2-0006) with The University of Arizona. The authors wish to thank Professor Emeritus J.W.S. Hearle of University of Manchester Institute of Science and Technology, University of Glasgow, UK and Dr. Philip Cunniff of US Army Natick Soldier Center for insightful email and oral discussions, respectively.

References

Cheeseman, B.A., Bogetti, T.A., 2003. Ballistic impact into fabric and compliant composite laminates. Composite Structures 61, 161–173.

Cheng, M., Chen, W., 2003. Experimental investigation of the stress–stretch behavior of EPDM rubber with loading rate effects. International Journal of Solids and Structures 40 (18), 4749–4768.

Cunniff, P.M., Ting, J., 1999. Development of a numerical model to characterize the ballistic behavior of fabrics. In: Proceedings of the 18th International Symposium of Ballistics, San Antonio, Texas, pp. 814–821.

Dorfmann, A., Ogden, R.W., 2004. A constitutive model for the Mullins effect with permanent set in particle-reinforced rubber. International Journal of Solids and Structures 41 (7), 1855–1878.

Hadley, D.W., Ward, I.M., Ward, J., 1965. The transverse compression of anisotropic fibre monofilaments. Proceedings of the Royal Society of London A 285 (1401), 275–286.

Hearle, J.W.S., 2003. Emeritus Professor of Textile Technology, University of Manchester Institute of Science and Technology. Personal communication, 2003.

Johnson, G.R., Beissel, S.R., Cunniff, P.M., 1999. A computational model for fabrics subjected to ballistic impact. In: 18th International Symposium on Ballistics, San Antonio, TX, pp. 962–969.

Johnson, G.R., Beissel, S.R., Cunniff, P.M., 2002. A computational approach for composite materials subjected to ballistic impact. In: The 2nd International Conference on Structural Stability and Dynamics, Singapore.

Kaw, A.K., 1997. Mechanics of Composite Materials. CRC Press, Boca Raton, New York.

Kawabata, S., 1990. Measurement of the transverse mechanical properties of high-performance fibres. Journal of the Textile Institute 81 (4), 432–447.

Lim, C.T., Shim, V.P.W., Ng, Y.H., 2003. Finite-element modeling of the ballistic impact of fabric armor. International Journal of Impact Engineering 28, 13–31.

McEwen, E., 1949. Stresses in elastic cylinders in contact along Generatrix. The Philosophical Magazine 40, Seventh Series (303), 454–459.

Mullins, L., 1969. Softening of rubber by deformation. Rubber Chemistry and Technology 42, 339–362.

Ogden, R.W., 2001. Pseudo-elasticity and stress softening. In: Fu, Y.B., Ogden, R.W. (Eds.), Nonlinear Elasticity—Theory and Applications. Cambridge University Press, pp. 491–522.

Ogden, R.W., Roxburgh, D.G., 1999a. A pseudo-elastic model for the Mullins effect in filled rubber. Proceedings of the Royal Society of London A 455, 2861–2877.

Ogden, R.W., Roxburgh, D.G., 1999. An energy-based model for the Mullins effect. In: Dorfmann, A., Muhr, A. (Eds.), Constitutive Models for Rubber, pp. 23–28.

Parga-Landa, B., Hernandez-Olivares, F., 1995. An analytical model to predict impact behavior of soft armour. International Journal of Impact Engineering 16, 455–466.

Pinnock, P.R., Ward, I.M., Wolfe, J.M., 1966. The compression of anisotropic fibre monofilaments. II. Proceedings of the Royal Society of London A 291 (1425), 267–278.

Roylance, D.K., Wilde, A.F., Tocci, C., 1973. Ballistic impact of textile structures. Textile Research Journal 43, 34–41.

Roylance, D., Hammas, P., Ting, J., Chi, H., Scott, B., 1995. Numerical modeling of fabric impact. AD-Vol. 48, High Strain Rate Effects on Polymer, Metal and Ceramic Matrix Composites and Other Advanced Materials, ASME, pp. 155–160.
Shim, V.P.W., Lim, C.T., Foo, K.J., 2001. International Journal of Impact Engineering 25, 1–15.
Taylor Jr., W.J., Vinson, J.R., 1990. Modeling ballistic impact into flexible materials. AIAA Journal 28, 2098–2103.
Yang, H.H., 1992. Kevlar Aramid Fiber. John Wiley & Sons, New York, NY.